DALTON
FULL PAPER

Crystallisation of calcium phosphates under constant conditions with a double diffusion set-up

Fabian Peters and Matthias Epple*

Solid State Chemistry, Faculty of Chemistry, University of Bochum, D-44780 Bochum, Germany. E-mail: matthias.epple@ruhr-uni-bochum.de; Fax: (+49) 234-3214-558

Received 1st August 2001, Accepted 29th October 2001
First published as an Advance Article on the web 26th November 2001

The crystallisation of calcium phosphate (apatite) was studied under computer-controlled conditions using a double diffusion set-up: constant pH in both compartments and constant concentrations of calcium, phosphate and fluoride. The influence of fluoride concentration, pH, overall concentration and of additives (cholesterol, magnesium) on the crystal morphology was investigated. The crystallite shapes fell into two main categories: spheres and hexagonal prisms, depending on the supersaturation. This set-up provides a suitable way to simulate biological crystallisation processes *in vitro*.

Introduction

Calcium phosphates form the structural basis of hard tissues in vertebrates. Bone, teeth, and tendon are all examples of mineralised tissues that contain calcium phosphate as reinforcing mineral.[1–3] In almost all cases, calcium phosphate occurs as hydroxyapatite $Ca_5(PO_4)_3OH$ ("HAP") with some degree of substitution of cations and anions. The most prominent substituting ion is carbonate CO_3^{2-} that occupies phosphate positions (so-called "B-type carbonated apatite"). In humans, bone and teeth contain nanometer-sized crystals of such carbonated apatites.[1–3]

Another prominent ion that can easily substitute hydroxide positions is fluoride that gives fluoroapatite $Ca_5(PO_4)_3F$ ("FAP"). Fluoride can be incorporated from 0 to 100% into the hydroxyapatite lattice so that often fluorohydroxyapatite is encountered: $Ca_5(PO_4)_3(OH)_{1-x}F_x$ ($x = 0.1$). Fluoroapatite is of interest as a constituent of shark teeth and also in the outer layer of human teeth after brushing with fluoride-containing toothpaste.[1,2]

Besides this desired biological crystallisation of calcium phosphates, pathological crystallisation phenomena frequently occur in the body. Most notable is the whole range of stone formations (*e.g.* in the bladder, kidney, or gall-bladder) and heterotopic calcifications (*e.g.* in menisci, within arteries or on implanted artificial heart valves) that in many cases involve calcium phosphate precipitation. The underlying mechanisms of both desired biomineralisation and undesired pathological biomineralisation are still only poorly understood. In many cases (as in bone) cellular action probably dominates[4,5] whereas in pathological crystallisations, physicochemical mechanisms often appear to be dominant.[6] Note that blood serum and saliva are oversaturated with respect to calcium phosphate precipitation.[7] In any case, the precipitation is controlled by interactions between a crystallising inorganic phase and adsorbed organic molecules (like proteins, lipids, glycoconjugates, antibodies).[8–11] Consequently, there have been numerous attempts to simulate calcium phosphate crystallisation *in vitro* in order to understand this process *in vivo* (see, *e.g.* references 12–21). This is not possible by simply mixing solutions containing both ions as the rapid precipitation leads to irregular, unspecific crystal shapes.

Here we present an experimental set-up that combines the advantages of two established crystallisation methods: a "*constant composition double diffusion*" apparatus ("CCDD"). A slow crystallisation through a porous membrane is carried out under defined conditions, *i.e.* at constant pH and constant ion concentrations. This permits the simulation of biological crystallisation processes *in vitro*, as demonstrated in the following for calcium phosphate.

Results and discussion

For biomimetic crystallisation of calcium phosphate, there are two major crystallisation techniques: double diffusion and constant composition. The "*double diffusion*" ("DD") crystallisation set-up involves two reservoirs of solutions that each contain a part of an insoluble salt, *e.g.* Ca^{2+} on one side and PO_4^{3-} on the other side. In order to prevent rapid mixing, the solutions are separated by a membrane or a gel that slow down diffusion and rate of crystallisation. However, if the two solutions meet, precipitation will occur, either on or within the separating matrix. Thereby, the slower crystallisation leads to better-shaped crystals, and the effects of additives and matrix effects (like biomimetic templating)[9] can be conveniently studied.

In general, the double diffusion technique permits the study of crystallisation on a long time scale, *i.e.* over days, weeks or even months. Its drawback is the constantly changing environment, *i.e.* the depletion of the solutions of the constituting ions (Ca^{2+}, PO_4^{3-}) due to precipitation, leading to a changing supersaturation and possibly changes in the crystallisation mechanism. Earlier results of double diffusion experiments with calcium phosphates are comprised in Table 1. Inspection of the different morphological results shows that there is a strong difference in morphology between fluoroapatite and hydroxyapatite/octacalcium phosphate and also that the results strongly differ depending on the experimental conditions.

Nancollas realised early that more meaningful results are obtained if the crystallisation conditions are held constant throughout the experiment.[12,22] These parameters are primarily the concentrations of the reactants (calcium, phosphate) and the pH. In the case of calcium phosphates a decrease in pH is always observed during crystallisation as hydrogen phosphate ions ($H_2PO_4^-/HPO_4^{2-}$) are precipitated as phosphate ions (PO_4^{3-}), thereby releasing protons. Continuous monitoring and regulation of these parameters in solution is therefore a prerequisite to study, *e.g.*, the influence of crystallisation additives.

Table 1 Double diffusion experiments in the literature with calcium phosphate in biomimetic matrices (FAP = fluoroapatite; HAP = hydroxyapatite, OCP = octacalcium phosphate)

Source	*T* / °C	Concentration	Membrane	Time	pH	Product and morphologies
Kniep and Busch[17,29]	25	$[CaCl_2]$ = 133 mM, stoichiometric for FAP	Collagen	2 to 6 weeks	2.5–5.5 (initially)	FAP: elongated hexagonal prisms, dumb-bells, spheres; 100 to 400 μm diameter
Schwarz and Epple[20]	37	$[CaCl_2]$= 133 and 186 mM, stoichiometric for FAP	Microporous polyglycolide	7 to 26 days	4.8–6	FAP: elongated hexagonal prisms, dumb-bells and spheres; 3–60 μm diameter
Schwarz and Epple[20]	37	*simulated body fluid* with $[Ca^{2+}]$ = 5 mM[41]	Microporous polyglycolide	26 days	*ca.* 7	HAP: hexagonal terraces and prisms, 5 × 40 μm^2; spheres of *ca.* 50 μm diameter
Falini *et al.*[21]	20	$[Ca^{2+}] = [PO_4^{3-}]$ = 7.3 mM	Denatured collagen	6 h to 2 days	7.4 (initially)	thin irregular platelets of OCP, extension 5–10 μm; HAP cannot be excluded
Suvorova *et al.*[42]	37–40	$[Ca^{2+}] = [PO_4^{3-}]$ = 53.56 mM	Reservoir of aqueous KCl solution	1, 2, 3, 4 weeks; 5 months (also in space)	7.4 (initially)	HAP and OCP; platelets and needles of several μm extension and tens of nm thickness
Iijima *et al.*[43]	37 °C	$[Ca^{2+}] = [PO_4^{3-}]$ = 7.2 mM	Slice of Achilles tendon of cow	1 day	6.5; 7; 7.4 (initially)	OCP and HAP: interwoven platelets of 1–10 μm extension

Nancollas proposed the "*Constant composition technique*" ("CC") in which the pH of an oversaturated calcium phosphate solution is monitored. Upon addition of seed crystals of calcium phosphate, crystallisation is induced. The resulting pH drop triggers the addition of OH^-, Ca^{2+} and $H_2PO_4^-$ so that, under the assumption of a stoichiometric hydroxyapatite precipitation, the concentrations of these ions in solution remain constant. By this technique, the influence of additives on the rate of (secondary) crystallisation can be studied.[12,22] Further experiments along this line were carried out by Gilman and Hukins who studied the influence of human serum albumin on the crystallisation of hydroxyapatite under constant conditions.[15] The drawback of this technique is the comparatively fast crystallisation (experimental times ranging from minutes to hours) that is not very close to biological systems where crystallisation usually occurs during days, weeks, months or years.

As a combination of both techniques, a "*constant composition double diffusion*" set-up ("CCDD") was constructed and tested for calcium phosphate crystallisation. The CCDD device consists of two thermostatted vessels that are separated by a membrane or a pellet. As diffusion constraint we used a pellet of (hydrophilic) microporous polyglycolide.[23] One vessel contains the calcium component, $Ca(NO_3)_2$, the other one the phosphate component, KH_2PO_4, and, if applicable, the fluoride component, KF. Note that potassium is incorporated into hydroxyapatite to a much lesser extent than sodium.[2] The use of calcium chloride as in references 17,20 was avoided as chloride may also be incorporated yielding a non-stoichiometric chloroapatite.[2]

The pH is continuously monitored on each side. A decrease from the pre-set value on either side triggers one of two peristaltic pumps to add KOH solution. Note that because in all crystallisation experiments the pH decreased by precipitation, it was never necessary to add acid. The calcium ion concentration is monitored in the corresponding vessel by an ion-selective calcium electrode. Deviations from the pre-set value trigger a peristaltic pump that simultaneously adds $Ca(NO_3)_2$ solution to the calcium side and KH_2PO_4 solution to the phosphate side (in the stoichiometric ratio 5 : 3 for apatite). Fig. 1 shows a schematic set-up of the apparatus.

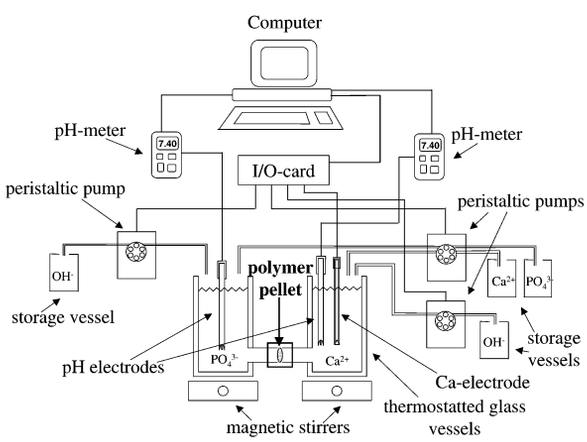

Fig. 1 Schematic set-up of the CCDD apparatus. The apparatus consists of two vessels that are connected by a porous membrane and controlled by two pH meters and one calcium ion-selective electrode. In case of a deviation from the pre-set values, the depleted ions are added by three peristaltic pumps. The whole system is thermostatted and controlled by a computer.

After the pre-set time (7 d at 37 °C, unless otherwise noted), the polymer pellet was removed and studied by scanning electron microscopy (SEM) and (in some cases) by synchrotron X-ray powder diffraction. It turned out necessary to employ this radiation source as the amount of precipitated crystals was generally small compared to the semi-crystalline polymer matrix. The calcium phosphate was identified as being

exclusively apatite in all cases (*i.e.* no octacalcium phosphate, OCP, $Ca_8(HPO_4)_2(PO_4)_4{\cdot}5H_2O$, or any other calcium phosphate phase). IR spectroscopy that is often very useful to identify calcium phosphates[24] was not possible due to the small proportion of calcium phosphate in the polymeric matrix. Both sides of the pellet and its interior were studied separately by SEM. The crystallisation occurred mostly on the phosphate-side of the pellet, indicating that calcium diffused much faster through the membrane than phosphate.

Before going into the details, we want to stress that all results were obtained at different areas of each sample or on different samples that underwent the same treatment. None of the reported results or the shown morphologies is a "singular event" that was observed only once.

Crystallisation of hydroxyapatite

At first, we precipitated hydroxyapatite from solutions in the stoichiometric ratio: $[Ca^{2+}]$ = 66.5 mM, $[PO_4^{3-}]$ = 40 mM, at physiological pH (7.4). The typical morphology of hydroxyapatite was found, *i.e.* spherical aggregates composed of platelet-like hydroxyapatite crystals that are interwoven into a porous structure. Fig. 2 shows two illustrative pictures.

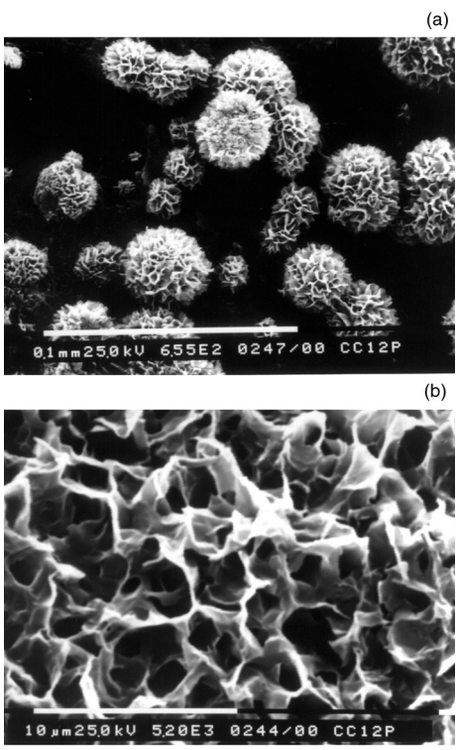

Fig. 2 Hydroxyapatite crystals precipitated on the surface of the pellet (phosphate side) at pH 7.4 ($[Ca^{2+}]$ = 66.5 mM, $[PO_4^{3-}]$ = 40 mM). Note the typical spherical aggregates (a) that consists of fused platelet-like subunits (b).

Very similar pictures were reported earlier for hydroxyapatite crystallised on metal and ceramic surfaces.[25–27]

Crystallisation of hydroxyapatite with variable fluoride concentration

Fluoride ions are easily incorporated into the hydroxyapatite lattice. Solid solutions ranging from pure hydroxyapatite to pure fluoroapatite can be formed. Fluoride induces crystallisation and also lowers the solubility under acidic conditions. This effect is well known in dentistry (fluoride in toothpaste) and in bone biology (prevention of osteoporosis by administration of fluoride).[28] Because an unusual crystal morphology for fluoroapatite in collagen was reported by Kniep and Busch (elongated hexagonal prisms expanding into dumb-bells and finally spheres),[17,29] it appeared to be interesting to investigate the influence of fluoride concentration. Iijima *et al.* studied the effect of small amounts of fluoride upon the crystallisation of calcium phosphate. He found that the presence of larger amounts of fluoride induces the crystallisation of hydroxyapatite instead of octacalcium phosphate.[30]

We have therefore studied the crystallisation of fluorohydroxyapatite at variable fluoride concentration at pH 7.4, $[Ca^{2+}]$ = 66.5 mM and $[PO_4^{3-}]$ = 40 mM. For stoichiometric fluoroapatite, $Ca_5(PO_4)_3F$, a molar ratio of Ca : F of 5 : 1 would be required. In order to elucidate the influence of the fluoride concentration on the crystal morphology, we have run experiments at Ca : F ratios of 5 : 0 (see the preceding section, *i.e.* pure hydroxyapatite), 5 : 0.33, 5 : 0.67 and 5 : 1.

Even a small amount of fluoride (Ca : F = 5 : 0.33) considerably changes the morphology of the crystallites. There are still spherical aggregates, but they do not consist of platelets anymore but rather have an "exploded" appearance (Fig. 3). Inside

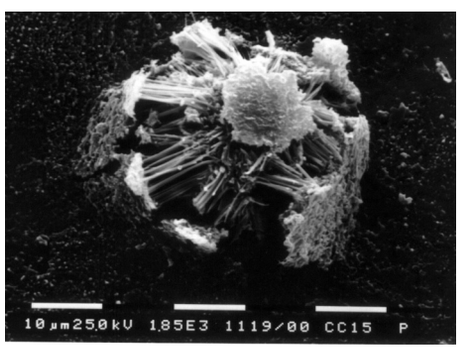

Fig. 3 Crystallisation of fluorohydroxyapatite at pH 7.4 at a concentration ratio of Ca : F = 5 : 0.33 ($[Ca^{2+}]$ = 66.5 mM, $[PO_4^{3-}]$ = 40 mM).

these pseudo-spherical aggregates, the platelets are still visible. Apparently, the system is on the edge of the choice between these two crystal morphologies. At higher fluoride concentration (Ca : F = 5 : 0.67), associated compact spheres were observed (Fig. 4). The morphology of crystals from a stoichio-

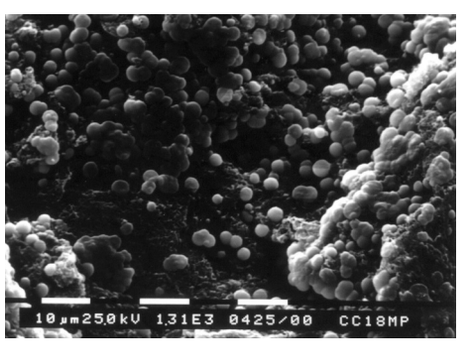

Fig. 4 Crystallisation of fluorohydroxyapatite at pH 7.4 at a concentration ratio of Ca : F = 5 : 0.67 ($[Ca^{2+}]$ = 66.5 mM, $[PO_4^{3-}]$ = 40 mM).

metric fluoroapatite solution (Ca : F = 5 : 1) strongly depended on the location within the polymer pellet. On the surface of the phosphate side, we found a layer of elongated prisms starting to branch out at both ends (Fig. 5a). Below, *i.e.* within the pellet, elongated hexagonal prisms with a length of about 9–11 μm occurred (Fig. 5b). Moving on towards the calcium side, the length of the prisms increased to 14–20 μm and spheres (diameter 10–12 μm) were found (Fig. 5c). Farther towards the calcium side, the hexagonal prisms vanished and only spheres of 5–6 μm diameter were present (Fig. 5d). There is no conceivable way to relate the prismatic morphology with the spherical morphology. We may therefore conclude that there are two different crystal growth mechanisms for fluoroapatite: one resulting in a linear growth along the hexagonal *c*-axis and one

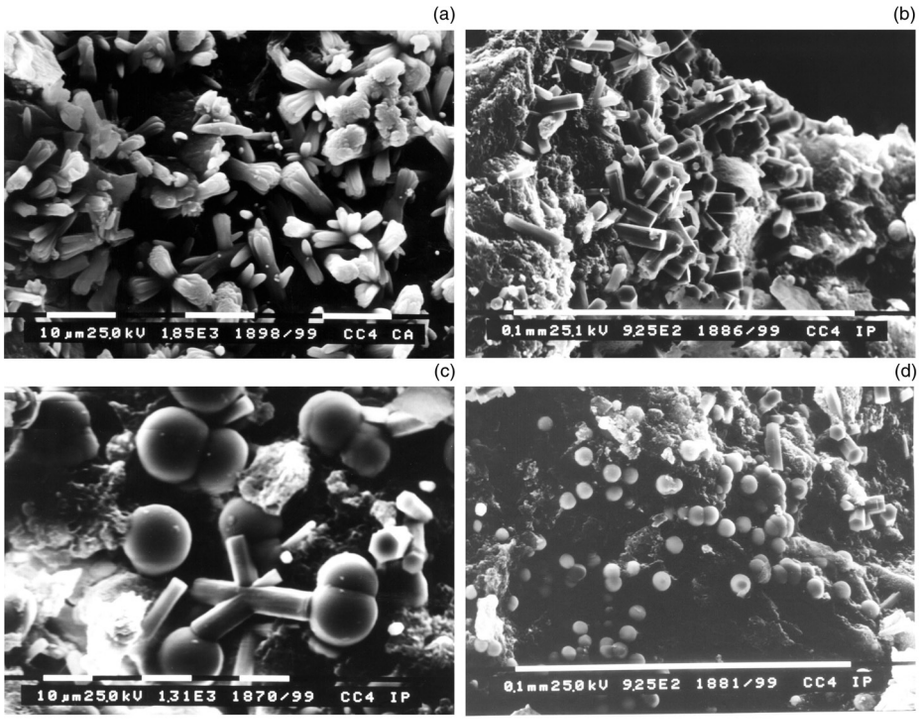

Fig. 5 Crystallisation of fluoroapatite at pH 7.4 at a stoichiometric concentration ratio of Ca : F = 5 : 1 ($[Ca^{2+}] = 66.5$ mM, $[PO_4^{3-}] = 40$ mM), going from the surface on the phosphate side (a) towards the calcium side (b through d).

% Fluoride	0	33	67	100
Ca : F	5 : 0	5 : 0.33	5 : 0.67	5 : 1
Surface Phosphate Side	general shape, 3-4 µm, 10-32 µm	35 µm, 5-6 µm irregular	7.5-14 µm irregular	9-11 µm, 2-5 µm
Interior Phosphate Side	**no crystal formation**	**no crystal formation**	1-5 µm regular	14-20 µm, 4-6 µm, 10-12 µm

Fig. 6 Schematic representation of all aggregates found at different fluoride concentration (7 d, pH 7.4, $[Ca^{2+}] = 66.5$ mM, $[PO_4^{3-}] = 40$ mM).

resulting in isotropic, spherical growth. All morphological results are comprised in Fig. 6.

Crystallisation of fluoroapatite at different supersaturation

The supersaturation is a decisive quantity for the crystallisation mechanism.[31] In non-controlled crystallisation experiments (like non-controlled double-diffusion experiments), the concentration of the reactants (and thereby the supersaturation) continuously decreases, therefore a change in the crystallite morphology could occur unnoticed during an experiment. Consequently, we have studied the crystallisation of fluoroapatite from stoichiometric solutions ($Ca : PO_4 : F = 5 : 3 : 1$) but at different overall concentrations: $[Ca^{2+}] = 66.5$ mM, 99.75 mM and 133 mM (with the concentrations of phosphate and fluoride adjusted accordingly). The results for $[Ca^{2+}] = 66.5$ mM were already discussed in the preceding paragraph (Ca : F = 5 : 1).

At $[Ca^{2+}] = 99.75$ mM we found intergrown, but well-shaped, regular hexagonal prisms that appeared to result from a single nucleus. The same prisms and spheres as at $[Ca^{2+}] = 66.5$ mM were also found, but generally with smaller size (Fig. 7). At 133 mM $[Ca^{2+}]$ we found an additional feature: open spheres that indicated a radial crystal growth with onion-like morphology (Fig. 8). Fig. 9 summarises all results that were obtained for experiments at variable overall concentration. By synchrotron X-ray diffraction, the phases formed could be clearly identified as apatite. Note that it is very difficult to distinguish between hydroxyapatite and fluoroapatite by diffraction as the lattice constants are almost identical (HAP: $a = 9.424$, $c = 6.876$ Å;[32] FAP: $a = 9.367$, $c = 6.884$ Å).[33]

The crystallisation occurred mainly on the phosphate side, indicating a fast diffusion of calcium through the matrix to the phosphate side, where the crystallisation occurred. This leads to a high supersaturation on the phosphate-side of the matrix that decreases towards the calcium side. Thus, we can assume a gradient in the nucleation rate from the surface of the phosphate side (high) towards the interior (lower). At high supersaturation, many nuclei and therefore many smaller crystals are expected, whereas at lower supersaturation, fewer nuclei and

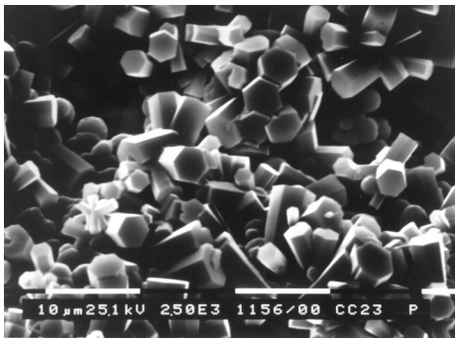

Fig. 7 Fluoroapatite from experiments at 1.5 times standard concentration (pH 7.4, Ca : F = 5 : 1, $[Ca^{2+}]$ = 99.75 mM, $[PO_4^{3-}]$ = 60 mM) on the surface of the phosphate side.

Fig. 8 Hollow spheres of fluoroapatite crystallised on the surface of the phosphate side from experiments at two times standard concentration (pH 7.4, Ca : F = 5 : 1, $[Ca^{2+}]$ = 133 mM, $[PO_4^{3-}]$ = 80 mM).

less but larger crystals should be formed. With increasing overall concentration, the supersaturation increases as well. These considerations explain the formation of smaller prisms and spheres inside the pellet and the growth of interconnected prisms on the surface at higher concentration (99.75 *vs.* 66.5 mM). If the supersaturation is very high (surface at 133 mM), the spheres appear to adopt secondary and tertiary layers of crystallites leading to the special onion-like morphology. Prisms are not formed at this high supersaturation whereas spheres occur under almost all conditions.

Crystallisation of fluoroapatite at variable pH

The precipitation of apatite generally leads to a decrease of pH as hydrogen phosphate is precipitated as phosphate (eqn. 1). The actual amount of H^+ release depends on the pH (hydrogen phosphate/dihydrogen phosphate equilibrium) and on the amount of fluoride incorporation (more or less OH^- being

$$5\ Ca^{2+} + 3\ HPO_4^{2-} + H_2O \longrightarrow Ca_5(PO_4)_3OH + 4\ H^+ \quad (1)$$

incorporated into the precipitate). In any case, under non-controlled conditions the pH decreases and therefore the precipitation conditions are not stationary. The solubility of apatites increases at low pH, a fact that is exploited by osteoclasts,[34] the bone-resorbing cells that create an acidic environment on the bone surface, or by bacteria during caries attack on teeth.

We have studied the precipitation of fluoroapatite at pH values of 5, 6, 7.4 (as described above), and 9 at the standard concentration of $[Ca^{2+}]$ = 66.5 mM (stoichiometric composition for fluoroapatite). As in the previous experiments, crystallisation occurred mainly on the surface of the pellet on the phosphate side. At pH 5, we found small spheres of 0.4–1.5 µm diameter (Fig. 10). At pH 6, the aggregates were larger and less regular (0.9–2.3 µm) and there were first indications of elongated prisms (Fig. 11). In alkaline medium, at pH 9, we found only spherical aggregates (Fig. 12). At this high pH, we also

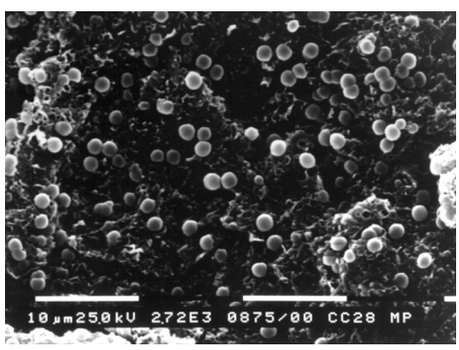

Fig. 10 Fluoroapatite crystallised at pH 5 from stoichiometric solution (Ca : F = 5 : 1) inside the pellet towards the phosphate side ($[Ca^{2+}]$ = 66.5 mM, $[PO_4^{3-}]$ = 40 mM).

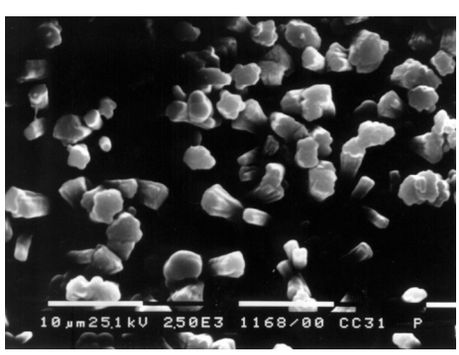

Fig. 11 Fluoroapatite crystallised at pH 6 from stoichiometric solution (Ca : F = 5 : 1) on the surface of the phosphate side ($[Ca^{2+}]$ = 66.5 mM, $[PO_4^{3-}]$ = 40 mM).

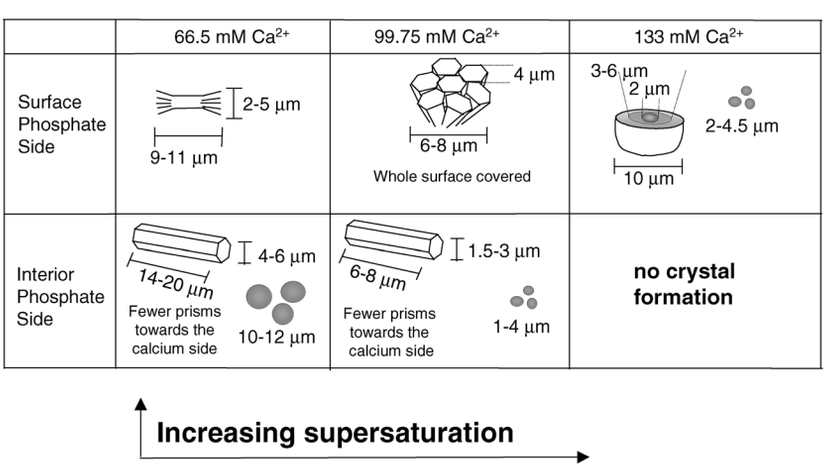

Fig. 9 Schematic representation of all crystal shapes that were found at variable overall concentration at stoichiometric fluoroapatite ratio (7 d, pH 7.4, Ca : PO_4 : F = 5 : 3 : 1).

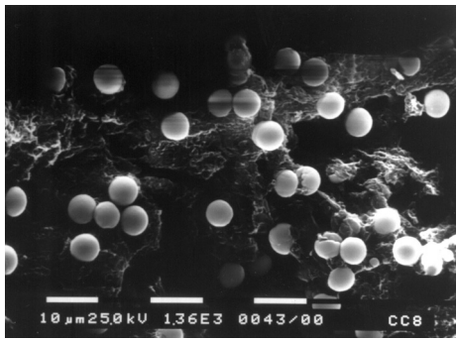

Fig. 12 Fluoroapatite crystallised at pH 9 from stoichiometric solution (Ca : F = 5 : 1) inside the pellet towards the phosphate side ($[Ca^{2+}] = 66.5$ mM, $[PO_4^{3-}] = 40$ mM).

observed precipitation of calcium carbonate (calcite) as detected by X-ray diffraction. Note that the crystallisation vessels could not be completely closed to prevent access of air (and thereby CO_2).

Fig. 13 summarises the results of the crystallisation experiments at different pH. The supersaturation increases with increasing pH. We found only spheres at very high supersaturation and any elongated aggregates only at medium supersaturation. The size of the omnipresent spheres decreased with decreasing pH.

pH	5	6	7.4	9
Surface Phosphate Side	0.4-1 µm	1-2.3 µm, 4-5 µm, 1.4-3 µm	9-11 µm, 2-5 µm	4.5-6.5 µm
Interior Phosphate Side	1-1.5 µm	no crystal formation	14-20 µm, 4-6 µm, 10-12 µm	0.8-14 µm

Fig. 13 Schematic representation of all crystal shapes of fluoroapatite found at different pH (7 d, Ca : PO_4 : F = 5 : 3 : 1).

Crystallisation in the presence of additives

Biological crystallisation is usually under strict control of substances that can adsorb on specific crystal faces and thereby influence nucleation and growth of the crystals.[31,35,36] Such interactions can be conveniently studied with the present set-up. As a striking example, we have studied the crystallisation of hydroxyapatite in the presence of cholesterol, a compound that is well known to occur in association with hydroxyapatite in atherosclerotic lesions.[11,37,38]

The morphology of hydroxyapatite was strongly altered by the presence of cholesterol (saturated solution, solubility about 2 mg l^{-1}, 7 d, pH 7.4, $[Ca^{2+}] = 66.5$ mM, $[PO_4^{3-}] = 40$ mM). In contrast to the highly porous aggregates composed of thin platelets, we found compact spheres with a diameter of about 5–10 µm (Fig. 14). These aggregates resemble those found in explanted atherosclerotic lesions.[39] It should be emphasised that this is not proof of an interaction between the growing hydroxyapatite crystal and dissolved cholesterol that is identical to the biological system, but the result demonstrates that it is possible to study the influence of additives on crystallite morphology.

A second experiment was done with magnesium that is well known to influence the morphology of apatite crystals.[40] In the presence of magnesium in a 1 : 1 ratio to calcium (7 d, pH 7.4, $[Ca^{2+}] = 66.5$ mM, $[Mg^{2+}] = 66.5$ mM, $[PO_4^{3-}] = 40$ mM), we found an inhibited crystallisation with only few crystals of sizes of about 1 µm. Fig. 15 comprises some illustrative results.

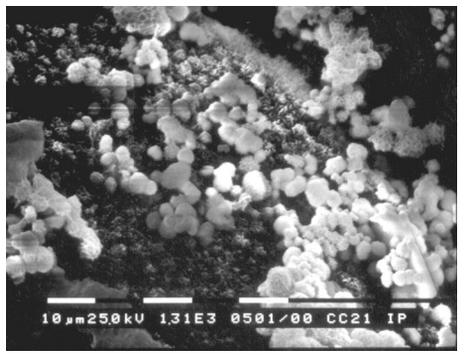

Fig. 14 Hydroxyapatite crystallised on the surface of the phosphate side in the presence of a saturated cholesterol solution, forming aggregates that resemble atherosclerotic lesions (pH 7.4, $[Ca^{2+}] = 66.5$ mM, $[PO_4^{3-}] = 40$ mM).

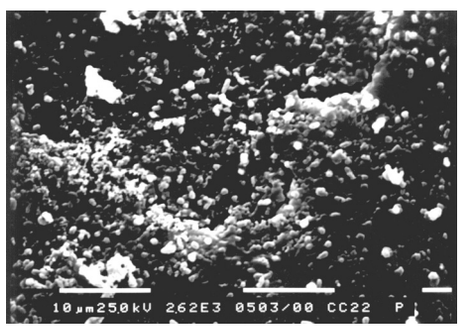

Fig. 15 Hydroxyapatite crystallised on the surface of the phosphate side in the presence of magnesium (pH 7.4, $[Ca^{2+}] = 66.5$ mM, $[Mg^{2+}] = 66.5$ mM, $[PO_4^{3-}] = 40$ mM).

Conclusions

The experiments have shown that a combination of the techniques of double diffusion and constant composition permits a well-defined crystallisation. Nevertheless, local variations in concentration may still occur even within a thin crystallisation matrix leading to variable oversaturation and consequently different rates of nucleation. Therefore, different crystal morphologies are found within a single polymer pellet, mostly as a function of depth. However, the crystal shapes and sizes are far more uniform within a single crystallisation "layer" than under non-controlled conditions.

Fig. 16 comprises in condensed form all results obtained for the crystallisation of fluoroapatite as a function of oversaturation. Spheres appear to be formed at any oversaturation with decreasing diameter at higher supersaturation. Prisms,

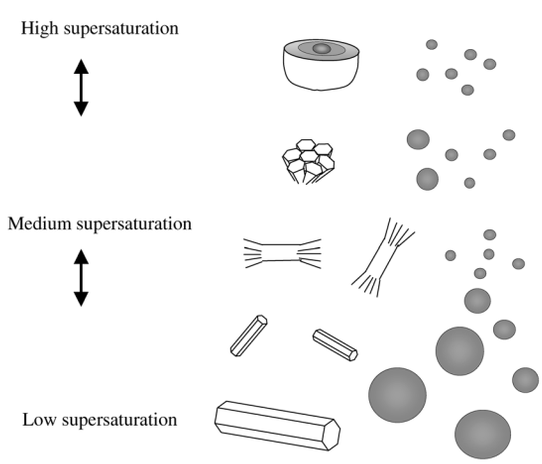

Fig. 16 Systematic representation of crystallisation pathways for fluoroapatite as a function of supersaturation.

dumb-bells and multi-shell spheres are formed only in distinct concentration regions. As the time of our experiments was generally shorter than at the earlier experiments that reported fractal crystal growth leading from dumb-bells to closed spheres (7 days *vs.* several weeks),[17,20,29] it may be speculated that longer experiments would also show this special crystal morphology.

In summary, the following conclusions can be drawn: (i) The hydroxyapatite morphology is influenced by small amounts of fluoride (platelet morphology is changed to spherical or prismatic). (ii) Different growth mechanisms of fluoroapatite exist at different oversaturation (spheres and prisms). (iii) Hexagonal prisms of fluoroapatite have a typical ratio of length to diameter of *ca.* 4 : 1 in all cases (comparing well to 5 : 1 reported earlier).[29] (iv) Branching to dumb-bells occurs only under specific conditions of supersaturation and pH. (v) A decreasing pH leads to smaller crystals of fluoroapatite. For instance, spheres are smaller. (vi) Cholesterol and magnesium influence the crystallisation of hydroxyapatite by adsorption and/or incorporation.

The fact that crystallisation mostly occurred on the surface of the pellets makes it likely that a templating interaction between the matrix (polyglycolide) and the precipitate (apatite) is not of decisive influence. There may be a nucleating effect on the surface, but the crystal morphology in later stages is probably controlled only by the surrounding solution, *i.e.* by the local supersaturation. Experiments are currently being carried out to replace the polyglycolide membrane by a fully inert membrane.

The presented apparatus has been shown to achieve a significant improvement in crystallisation methods, especially when the effect of crystallisation admixtures has to be tested. Although its applicability was demonstrated for the case of a typical biomineral and biomaterial (calcium phosphate), the set-up is principally suitable for all precipitation reactions that can be performed by mixing two solutions containing the components of the precipitate (like $CaCO_3$, $BaSO_4$, or sulfides).

Experimental

The schematic set-up of the CCDD device is shown in Fig. 1. A porous polymer pellet (solid-state chemically prepared polyglycolide from sodium chloroacetate with about 42 % porosity and pores of 0.2–0.3 μm size serves as membrane between two thermostatted glass vessels that contain aqueous $Ca(NO_3)_2$ and K_2HPO_4, respectively. The pH is initially adjusted to the pre-set value (*e.g.*, 7.4) on both sides by addition of HNO_3. Diffusion of the solutions leads to precipitation of calcium phosphate on or within the polymer pellet. Two pH meters (WTW PH 340-A) and one calcium-sensitive electrode (ORION 97-20 ion plus combination electrode) continuously monitor the concentrations of H^+ and Ca^{2+} in the vessels. Three peristaltic pumps (Ismatec Reglo Analog, MS-2/6-160) are triggered by any deviation of the three concentrations from their pre-set values. The pH is maintained by addition of aqueous KOH. The calcium concentration is maintained by addition of calcium nitrate to the calcium side of the apparatus. We assumed a crystallisation of calcium phosphate in the stoichiometric ratio of hydroxyapatite, $Ca_5(PO_4)_3OH$, *i.e.* 5 : 3 (Ca/P = 1.67), and simultaneously added a pH-adjusted solution of K_2HPO_4 to the vessel containing phosphate. In case of the precipitation of fluoroapatite, pH-adjusted KF solution was also added to the phosphate side in the corresponding stoichiometric ratio. The accuracy of the control over the concentrations of Ca^{2+} and PO_4^{3-} was checked on aliquots taken that were analysed by atomic absorption spectroscopy for calcium and photometry for phosphate, as molybdovanadate complex.

This apparatus is able to keep the conditions within the following ranges: pH (calcium side; at 7.4): ±0.05, pH (phosphate side; at 7.4): ±0.02, $c(Ca^{2+}$; at 66.5 mM): ±10 mM; $c(PO_4^{3-}$; at 40 mM): ±6 mM; temperature $T = 37 \pm 0.3$ °C. The control over all parameters and continuous monitoring on a time scale of 0.1 s (Ca^{2+}) to 1 s (pH) was done by a computer using serial interfaces (RS 232) and an AD/DA conversion card. Internally, the computer used self-programmed routines of the program VISIDAQ (Advantech). All electrodes were thoroughly calibrated before the experiments. Despite different attempts, it was not possible to compute the rate of crystallisation from the volumes added to the vessels. This is due to the diluting effect of the added base that mainly triggers the addition of calcium and phosphate. The amount of precipitate apparently is too small to be separated from this effect.

All experiments were carried out with demineralised water. All solutions were prepared with compounds of *pro analysi* quality obtained from Merck.

Acknowledgements

We thank the Deutsche Forschungsgemeinschaft and the Fonds der Chemischen Industrie for generous financial support and HASYLAB at DESY (Hamburg) for allocation of beamtime.

References

1 H. A. Lowenstam and S. Weiner, *On biomineralization*, Oxford University Press, Oxford, 1989.
2 R. Z. LeGeros, in *Biological and synthetic apatites*, ed. P. W. Brown and B. Constantz, CRC Press, Boca Raton, 1994.
3 S. Weiner and H. D. Wagner, *Annu. Rev. Mater. Sci.*, 1998, **28**, 271.
4 U. Plate, T. Kotz, H. P. Wiesmann, U. Stratmann, U. Joos and H. J. Höhling, *J. Microsc.*, 1996, **183(7)**, 102.
5 U. Stratmann, K. Schaarschmidt, H. P. Wiesmann, U. Plate and H. J. Höhling, *Cell Tissue Res.*, 1996, **284**, 223.
6 W. Jahnen-Dechent, T. Schinke, A. Trindl, W. Muller-Esterl, F. Sablitzky, S. Kaiser and M. Blessing, *J. Biol. Chem.*, 1997, **272**, 31496.
7 M. Epple and P. Lanzer, *Z. Kardiol.*, 2001, **90:Suppl.3**, III/2.
8 L. Addadi and S. Weiner, *Angew. Chem.*, 1992, **104**, 159.
9 S. Mann, *Biomimetic materials chemistry*, VCH, Weinheim, 1996.
10 S. Weiner and L. Addadi, *J. Mater. Chem.*, 1997, **7**, 689.
11 D. Izhaky and L. Addadi, *Chem. Eur. J.*, 2000, **6**, 869.
12 P. Koutsoukos, Z. Amjad, M. B. Tomson and G. H. Nancollas, *J. Am. Chem. Soc.*, 1980, **102**, 1553.
13 C. S. Sikes, M. L. Yeung and A. P. Wheeler, in *Surface reactive peptides and polymers: Discovery and commercialization*, ACS Symposium Series, 1991, vol. 444, pp. 50–71.
14 S. I. Stupp and G. W. Ciegler, *J. Biomed. Mater. Res.*, 1992, **26**, 169.
15 H. Gilman and D. W. L. Hukins, *Inorg. Biochem.*, 1994, **55**, 21.
16 P. W. Brown and M. Fulmer, *J. Biomed. Mater. Res.*, 1996, **31**, 395.
17 R. Kniep and S. Busch, *Angew. Chem.*, 1996, **108**, 2788.
18 G. A. Ozin, N. Varaksa, N. Coombs, J. E. Davies, D. D. Perovic and M. Ziliox, *J. Mater. Chem.*, 1997, **7**, 1601.
19 T. Kokubo, *Acta Mater.*, 1998, **46**, 2519.
20 K. Schwarz and M. Epple, *Chem. Eur. J.*, 1998, **4**, 1898.
21 G. Falini, M. Gazzano and A. Ripamonti, *J. Mater. Chem.*, 2000, **10**, 535.
22 M. B. Tomson and G. H. Nancollas, *Science*, 1978, **200**, 1059.
23 M. Epple and O. Herzberg, *J. Mater. Chem.*, 1997, **7**, 1037.
24 C. Rey, V. Renugopalakrishnan, B. Collins and M. J. Glimcher, *Calcif. Tissue Int.*, 1991, **49**, 251.
25 S. B. Cho, K. Nakanishi, T. Kokubo, N. Soga, C. Ohtsuki and T. Nakamura, *J. Biomed. Mater. Res.*, 1996, **33**, 145.
26 H. B. Wen, Q. Liu, J. R. de Wijn, K. de Groot and F. Z. Cui, *J. Mater. Sci. Mater. Med.*, 1998, **9**, 121.
27 H. M. Kim, H. Takadama, T. Kokubo, S. Nishiguchi and T. Nakamura, *Biomaterials*, 2000, **21**, 353.
28 M. D. Grynpas and P. T. Cheng, *Bone & Mineral*, 1988, **5**, 1.
29 S. Busch, H. Dolhaine, A. DuChesne, S. Heinz, O. Hochrein, F. Laeri, O. Podebrad, U. Vietze, T. Weiland and R. Kniep, *Eur. J. Inorg. Chem.*, 1999, 1643.
30 M. Iijima, D. G. A. Nelson, Y. Pan, A. T. Kreinbrink, M. Adachi, T. Goto and Y. Moriwaki, *Calcif. Tissue Int.*, 1996, **59**, 377.
31 J. Nyvlt and J. Ulrich, *Admixtures in Crystallisation*, VCH, Weinheim, 1995.

32 K. Sudarsanan and R. A. Young, *Acta Crystallogr., Sect. B*, 1969, **24**, 1534.
33 K. Sudarsanan, P. E. Mackie and R. A. Young, *Mater. Res. Bull.*, 1972, **7**, 1331.
34 S. L. Teitelbaum, M. M. Tondravi and F. P. Ross, *J. Leucocyte Biol.*, 1997, **61**, 381.
35 J. Aizenberg, S. Albeck, S. Weiner and L. Addadi, *J. Cryst. Growth*, 1994, **142**, 156.
36 S. Albeck, S. Weiner and L. Addadi, *Chem. Eur. J.*, 1996, **2**, 278.
37 H. C. Stary, *Z. Kardiol.*, 2000, **89:Suppl. 2**, II/28.
38 B. B. Tomazic, *Z. Kardiol.*, 2001, **90:Suppl.3**, III/68.
39 B. B. Tomazic, in *Characterization of mineral phases in cardiovascular calcification*, ed. P. W. Brown and B. Constantz, CRC Press, Boca Raton, 1994.
40 M. H. Salimi, J. C. Heughebaert and G. H. Nancollas, *Langmuir*, 1985, **1**, 119.
41 O. P. Filho, G. P. LaTorre and L. L. Hench, *J. Biomed. Mater. Res.*, 1996, **30**, 509.
42 E. I. Suvorova, F. Christensson, H. E. Lundager Madsen and A. A. Chernov, *J. Cryst. Growth*, 1998, **186**, 262.
43 M. Iijima, Y. Morikawa, R. Yamaguchi and Y. Kuboki, *Conn. Tissue Res.*, 1997, **36**, 73.